Clinical and Translational Radiation Oncology 18 (2019) 46–53

Contents lists available at ScienceDirect

Clinical and Translational Radiation Oncology

journal homepage: www.elsevier.com/locate/ctro

Original Research Article

Individual lymph nodes: "See it and Zap it"

Dennis Winkel [*,1], Anita M. Werensteijn-Honingh [1], Petra S. Kroon, Wietse S.C. Eppinga, Gijsbert H. Bol, Martijn P.W. Intven, Hans C.J. de Boer, Louk M.W. Snoeren, Jochem Hes, Bas W. Raaymakers, Ina M. Jürgenliemk-Schulz

Department of Radiotherapy, University Medical Center, Utrecht, The Netherlands

ARTICLE INFO

Article history:
Received 22 March 2019
Revised 28 March 2019
Accepted 29 March 2019
Available online 30 March 2019

Keywords:
Radiotherapy
Lymph node oligometastases
MRI-guided radiotherapy
Online plan adaptation
MR-linac

ABSTRACT

Background and purpose: With magnetic resonance imaging (MRI)-guided radiotherapy systems such as the 1.5T MR-linac the daily anatomy can be visualized before, during and after radiation delivery. With these treatment systems, seeing metastatic nodes with MRI and zapping them with stereotactic body radiotherapy (SBRT) comes into reach. The purpose of this study is to investigate different online treatment planning strategies and to determine the planning target volume (PTV) margin needed for adequate target coverage when treating lymph node oligometastases with SBRT on the 1.5T MR-linac.

Materials and methods: Ten patients were treated for single pelvic or para-aortic lymph node metastases on the 1.5T MR-linac with a prescribed dose of 5x7Gy with a 3 mm isotropic GTV- PTV margin. Based on the daily MRI and actual contours, a completely new treatment plan was generated for each session (adapt to shape, ATS). These were compared with plans optimized on pre-treatment CT contours after correcting for the online target position (adapt to position, ATP). At the end of each treatment session, a post-radiation delivery MRI was acquired on which the GTV was delineated to evaluate the GTV coverage and PTV margins.

Results: The median PTV V_{35Gy} was 99.9% [90.7–100%] for the clinically delivered ATS plans compared to 93.6% [76.3–99.7%] when using ATP. The median GTV V_{35Gy} during radiotherapy delivery was 100% [98–100%] on the online planning and post-delivery MRIs for ATS and 100% [93.9–100%] for ATP, respectively. The applied 3 mm isotropic PTV margin is considered adequate.

Conclusion: For pelvic and para-aortic metastatic lymph nodes, online MRI-guided adaptive treatment planning results in adequate PTV and GTV coverage when taking the actual patient anatomy into account (ATS). Generally, GTV coverage remained adequate throughout the treatment session for both adaptive planning strategies. "Seeing and zapping" metastatic lymph nodes comes within reach for MRI-guided SBRT.

1. Introduction

In recent years, stereotactic body radiotherapy (SBRT) has developed into standard clinical care for patients with oligometastases in many centers [1–3]. Based on the oligometastatic disease paradigm [4], treatment of individual metastatic lesions is being used to treat patients with limited metastatic disease to postpone the start of systemic therapies and ideally improve the progression-free survival or overall survival without compromising the quality of life [1,5–7].

Experience with minimally invasive therapies such as stereotactic body radiotherapy (SBRT) as alternative to surgery has mainly been gained for inoperable patients with liver and lung oligometastases [8–13]. However, SBRT has since been incorporated in standard clinical care for lymph node and bone oligometastases [6,14,15] and is also being used for oligometastases located in adrenal glands [16,17]. The minimally invasive nature of SBRT can be an advantage compared with surgical resection [1,8], especially for small target structures such as metastatic lymph nodes.

With prostate specific membrane antigen positron emission tomography (PSMA-PET) small metastatic nodes can be detected in a very early stage with less than 10 mm and even less than 5 mm short axis diameter [18]. In the majority of patients treated with SBRT for oligometastatic lymph nodes, the affected nodes

* Corresponding author at: University Medical Center Utrecht, Department of Radiotherapy, Q.00.3.11, P.O. Box 85500, 3508 GA Utrecht, The Netherlands.
E-mail address: d.winkel-2@umcutrecht.nl (D. Winkel).
[1] These authors contributed equally to this work.

https://doi.org/10.1016/j.ctro.2019.03.004
2405-6308/

originate from prostate cancer and like the primary tumors, have a low alpha/beta ratio [19]. This is considered one of the reasons for responding very well to SBRT, with local control being achieved in 98.1% of patients in a pooled analysis [20]. For oligometastases from other origins, a biological effective dose >100 Gy is also thought to be beneficial for achieving local control [1], but this will require a higher dose per fraction. In general, toxicity for SBRT of lymph node oligometastases is reported being mild, with on average 3% acute grade 2, 1% late grade 2, 0.3% acute grade 3 and 0.4% late grade 3 toxicity [2]. For prostate cancer oligometastases, SBRT can delay the start of androgen deprivation therapy (ADT) with approximately 8–13 months [5,6], thereby hopefully maintaining the patient's quality of life and avoiding the side effects of ADT such as sexual dysfunction [21].

SBRT for oligometastases has mainly been applied with cone beam computed tomography (CBCT) linear accelerators (linacs) or CyberKnife, with fractionation schedules ranging from 5 × 5–10 Gy to 1 × 12–24 Gy [20]. Single fraction SBRT has been used in some centers, in several cases aided by fiducial marker implantation [22–26]. To our knowledge, peer reviewed reports on the accuracy of lymph node targeting with CBCT are lacking. However, in our own clinical routine about 30% of metastatic lymph node (as detected by diagnostic PET-CT and MRI) are poorly visible on CBCT [27]. Compared to CBCT, magnetic resonance imaging (MRI) provides superior visualization of soft tissue targets with metastatic lymph nodes being one example [28].

The combination of online MRI for target and organ at risk (OAR) delineation, full online treatment planning and MRI for position verification is realized in the 1.5T MR-linac (combined 1.5T MR scanner and linear accelerator, Unity, Elekta AB, Stockholm, Sweden) [29,30]. New treatment plans based on the actual anatomy as depicted on MRI can be generated for every treatment fraction and online position verification is based on MRI information. The anatomy can be visualized during radiotherapy delivery (beam-on MRI) and after radiation delivery. With these facilities on board seeing the metastatic nodes with MRI and zapping them with SBRT comes into reach, as does high dose single fraction SBRT without fiducial markers. Furthermore, the daily anatomy of nearby OAR can easily be taken into account for daily treatment planning [30], which may decrease treatment related toxicity and increase the number of patients eligible for single fraction treatments [27,31,32].

However, despite the expected gain there are still uncertainties with regard to 1.5T MR-linac treatments in general and for lymph node metastases SBRT in particular. The clinically used PTV margin is still based on experiences at CBCT-linac, intra-fraction analyses using diagnostic MRIs and MR-linac commissioning data. In addition, the quality of inter-fraction correction with the 1.5T MR-linac with the two distinct online planning workflows: 'adapt to position' (ATP) and 'adapt to shape' (ATS) has not been investigated based on clinical data. The dosimetric effects of these different planning strategies may significantly affect the treatment benefit of online MRI guidance.

The objective of this manuscript is to demonstrate how close we are to "See it and Zap it" when treating lymph node oligometastases in the pelvis and para-aortic region with SBRT on the 1.5T MR-linac. Focus will be on 1) the suitability of ATS and ATP for correcting for inter-fraction motion and 2) the feasibility of delivering the dose adequately with ATS and ATP with a pre-defined PTV margin of 3 mm.

2. Material and methods

2.1. Patient characteristics

Ten patients were treated for single pelvic lymph node oligometastases on the 1.5T MR-linac (Unity, Elekta AB, Stockholm, Sweden) at our institute between August 2018 and February 2019. The metastatic lymph nodes were located in the pelvic region for seven patients, the other three patients had para-aortic lymph nodes (at the levels of L2-Th12 vertebral bodies). The patients with para-aortic lymph nodes received a 4D CT to assess whether the breathing induced target motion amplitude was within limits. For eight patients, the metastatic nodes originated from prostate cancer and were detected using Gallium-68 PSMA PET scans. The primary tumor was rectal or esophageal cancer for two patients, diagnosis of these lymph nodes was based on 2-deoxy-2-fluor ine-18-fluoro-D-glucose PET ((18)FDG-PET). The metastatic lymph nodes were diagnosed within median 49 months [range 18–159] after initial diagnosis of the primary tumor. All patients have provided written informed consent for using their data as part of an ethics review board approved observational study. The median short-axis diameter of the metastatic lymph nodes was 7.5 mm [5.3–21.3 mm].

2.2. Clinical treatment

Pre-treatment preparation consisted of MR imaging followed by CT-based treatment planning using the anatomical information of the registered MRI. For pre-treatment CT scan acquisition a special table overlay was used to enable patient set-up using specific couch index points. By doing so the position of the patient along the length of the couch is known and reproducible between the CT scan and each MRI based treatment session [30]. To reduce eventual motion, patients with lymph node metastases in the pelvic region were immobilized using a vacuum mattress (BlueBAG, Elekta AB, Stockholm, Sweden) with both hands on the chest and the elbows along the body. The patients with affected nodes in the para-aortic region were treated whilst wearing an abdominal corset [33] with the arms along the body.

Nodal targets were treated with a GTV-PTV margin of 3 mm. For each patient, a seven-beam IMRT pre-treatment plan [34] was created using Monaco TPS (Elekta AB, Stockholm, Sweden), taking into account the presence of the 1.5T magnetic field. For patients treated with the arms along the body, beam angles were selected such that the beams would not traverse the arms. OAR dose was lowered as much as possible, while maintaining a sufficient PTV coverage of V_{35Gy} > 95% and a D_{max} between 120 and 135%. Clinical dose criteria for the OARs were based on the UK SABR consortium guidelines (2016) (Table 1).

With online MR imaging as provided in the 1.5T MRI-linac, the pre-treatment plan can be adapted by either 1) taking the new target position into account (adapt to position, ATP) and optimizing on the pre-treatment CT and contours after a rigid registration and translation or 2) using the new patient anatomy (adapt to shape, ATS) and optimizing on the daily image and adapted contours (Fig. 1). For our clinical treatments plan adaptation was performed using the ATS workflow. During each treatment session, a daily MRI was acquired. Contours were automatically deformed. If necessary, the contours of the target lymph node(s) and OARs within 2 cm of the PTV(s) were manually adapted by a radiation oncologist [30]. Based on the daily MRI and the adapted contours, a completely new treatment plan was generated using segment shape and weight optimization based on a newly optimized fluence [35]. Radiation delivery according to the new plan was performed after MRI based position verification.

After each treatment session offline assessment of the intra-fraction motion was performed by recalculating the GTV coverage on the actual anatomy as seen on the post-delivery MRI, which was acquired on average 31:03 ± 3:40 min after the online planning MRI. Contouring of the GTV on the post-delivery MRI was performed by a single observer. Inter-observer contouring varia-

Table 1
Clinical dose criteria.

Structure	Offline constraints (pre-treatment plan)	Online constraints
Planning target volume	$V_{35Gy} > 95\%$ $D_{0.1\ cm3} < 47.25$ Gy	$V_{35\ Gy} > 95\%$ $D_{0.1\ cm3} < 47.25$ Gy
Aorta	$V_{53Gy} < 0.5\ cm^3$	$V_{53Gy} < 0.5\ cm^3$
Bladder	$V_{38Gy} < 0.5\ cm^3$ $V_{18.3Gy} < 15\ cm^3$	$V_{38Gy} < 0.5\ cm^3$
Bowel bag + Colon	$V_{32Gy} < 0.5\ cm^3$ $V_{25Gy} < 10\ cm^3$	$V_{32Gy} < 0.5\ cm^3$
Duodenum + Stomach	$V_{35Gy} < 0.5\ cm^3$ $V_{25Gy} < 10\ cm^3$	$V_{35Gy} < 0.5\ cm^3$
Esophagus	$V_{34Gy} < 0.5\ cm^3$ $V_{27.5Gy} < 5\ cm^3$	$V_{34Gy} < 0.5\ cm^3$
Kidney	$V_{16.8Gy} < 67\%$	$V_{16.8Gy} < 67\%$
Nerve root + sacral plexus	$V_{32Gy} < 0.1\ cm^3$	$V_{32Gy} < 0.1\ cm^3$
Rectum + Sigmoid	$D_{max} < 40$ Gy $V_{32Gy} < 0.5\ cm^3$	$V_{32Gy} < 0.5\ cm^3$
Spinal cord	$D_{max} < 28$ Gy	$D_{max} < 28$ Gy
Ureter	$D_{max} < 40$ Gy	$D_{max} < 40$ Gy

tion is considered negligible for these small and well visible lesions.

2.3. Retrospective analyses

2.3.1. ATS versus ATP based plan adaptation

To investigate the suitability for correcting for inter-fraction motion the dosimetric impact of plan adaptation based on the new patient position (ATP) versus plan adaptation using the daily anatomic information and contours (ATS) was evaluated. An additional plan was retrospectively created for each treatment fraction using the ATP workflow with segment shape and weight optimization. Because the resulting dose-volume histogram parameters for an ATP plan are based on the pre-treatment CT contours and may essentially give a false representation of the actual situation, these plans have additionally been calculated on the daily MRI and contours. The GTV and PTV coverage was then compared for each of these 3 plans; the clinically delivered ATS plans, the ATP plans and the ATP plans calculated on the daily anatomy.

2.3.2. GTV target coverage analysis

To determine whether dose coverage was sufficient during treatment and if PTV margins were adequate, the GTV coverage for the clinically delivered (ATS) plans and the ATP plans was evaluated. This was done by evaluating the dose on both the online planning MRI, acquired at the start of the treatment fraction, as well as the post-delivery MRI, acquired after dose delivery.

2.3.3. PTV margin determination

The PTV margin was re-evaluated using data of these first 10 patients with single lymph node metastases treated on the MR-linac. The margin M_{PTV} required to ensure a minimum dose to the GTV of 35 Gy for 90% of the patients was calculated using the Van Herk recipe [37] given by

$$M_{PTV} = \alpha\Sigma + \beta\sigma - \beta\sigma_p$$

with $\alpha = 2.5$, $\beta = 0.84$ and $\sigma_p = 3.2$ mm. A β value of 0.84 was used assuming a stereotactic treatment with a plateau-prescription dose ratio of 1.25 and maximum short axis diameter of the GTV > σ. σp defines the standard deviation that describes the width of an idealized Gaussian penumbra for the total dose distribution in water, which was approximately valid because electron densities were assessed to electron density of water except for the bones [30]. $\sigma = \sqrt{\sigma_{intra}^2 + \sigma_p^2}$ defines the total random error and $\Sigma = \sqrt{\Sigma_{intra}^2 + \Sigma_{MV-MRI}^2 + \Sigma_{MRI}^2}$ the total systematic error. This recipe is still adequate for hypo-fractionated treatments when $\sigma_{intra} << \sigma_p$ [38] and the effective systematic and random errors are used [39]. Delineations errors were not taken into account assuming that the physician includes the GTV generously as had been decided by forehand. The different error sources were also assumed to be statistically independent and normally distributed.

Both $\Sigma_{MV\text{-}MRI}$ and Σ_{MRI} were based on 3D vector measurements in our clinic. The contributions to the systematic errors were

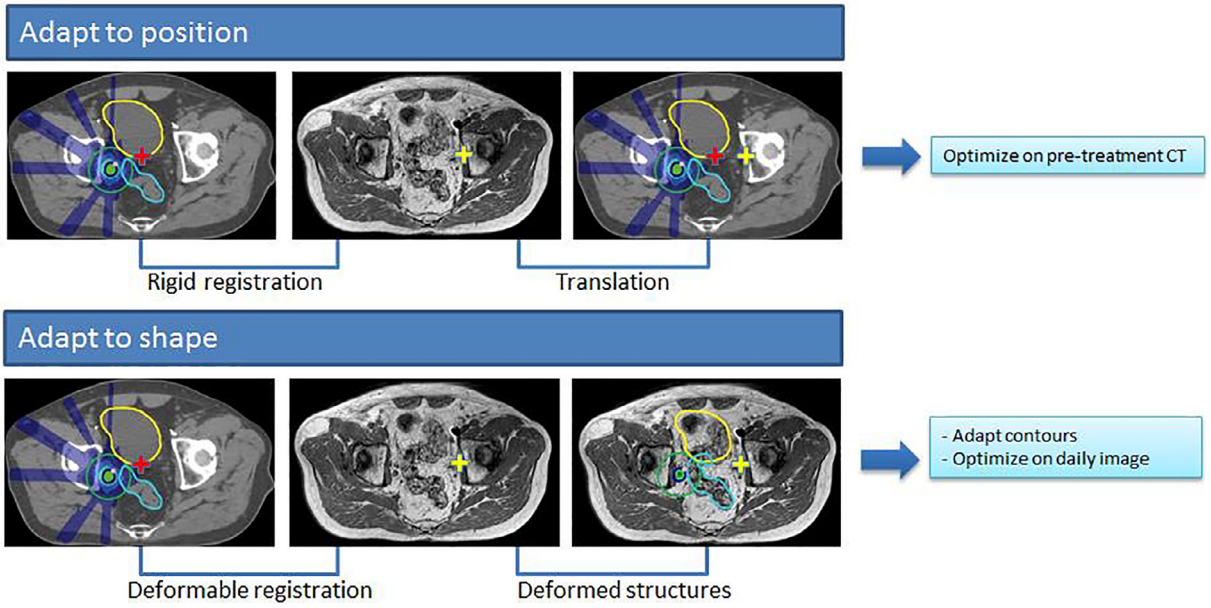

Fig. 1. Schematic overview of the differences between the MR-linac Unity "adapt to shape" method in which online plan adaptation is performed on the new patient anatomy and optimized on the daily MRI and adapted contours, and the "adapt to position" method in which online plan adaptation is performed based on the new patient position and optimized on the pre-treatment CT and contours. Using the "adapt to position" method, rigid registration can be performed on the entire image sets, or using a clipbox around a region of interest [36].

assumed isotrope. $\Sigma_{MV-MRI} = 0.3/\sqrt{3}$ mm was obtained from Raaymakers et al. [29] which defines the global error between the machine and MRI coordinate system. $\Sigma_{MRI} = 0.84/\sqrt{3}$ mm was determined during commissioning and describes the maximum residual geometric errors after gradient non-linearity correction within a 200 mm diameter spherical volume (DSV). This was measured on a large geometric fidelity phantom as described in Tijssen et al [40]. To obtain the systematic (Σ_{intra}) and random (σ_{intra}) group error due to intra-fraction motion, the distance in center of gravity of both GTV delineations, on the online MRI and post treatment MRI, was calculated for all five fractions of each patient. The intra-fraction deviations were then defined as the distance in center of gravity divided by two. The methodology given in Stroom and Heijmen. [41] was used to determine the group mean M (mean-of-means), systematic group error (defined as the standard deviation of the means) and random group error (defined as the root-mean-square of the standard deviations). The effective systematic error and effective random error were equal to the derived systematic and random error because the errors due to intra-fraction motion were already based on only 5 fractions. In case the group mean M significantly differed from zero, M was added to margin M_{PTV}.

3. Results

3.1. ATS versus ATP plan adaptation

The clinically delivered ATS plans show the highest PTV coverage with a median V_{35Gy} of 99.9% [90.7–100%] and GTV coverage with a median V_{35Gy} of 100% [99.7–100%]. For 9 fractions, PTV coverage was reduced during online planning to meet OAR constraints. The ATP plans, evaluated on the pre-treatment CT, also show sufficient target coverage with a median PTV V_{35Gy} of 98.5% [91.0–99.9%] and GTV V_{35Gy} of 100% for all fractions. However, after calculating the ATP plans on the new MRI based anatomy and contours, the PTV coverage is significantly lower (p-value < 0.01, Wilcoxon matched-pairs signed rank test) with a median PTV V_{35Gy} of 93.6% [76.3–99.7%] and a median GTV V_{35Gy} of 100% [93.9–100%]. Additionally, a larger variance between target coverage is observed (Fig. 2). If an OAR dose constraint violation occurred, the violation was with a maximum of 2 Gy or 0.2 cc for both methods.

3.2. GTV target coverage analysis

For the clinically delivered ATS plans the median GTV V_{35Gy} was 100% [99.7–100%] and the median GTV D_{mean} was 42.3 Gy [37.6–44.7 Gy] on the online planning MRI. On the post-radiation delivery MRI the median GTV V_{35Gy} was 100% [98.0–100%] and the median GTV D_{mean} was 42.2 Gy [37.9–44.7 Gy] (Fig. 3). For 45 of the 50 fractions (90%) the GTV V_{35Gy} on the post-delivery MRI remained 100%. For one patient, a slight reduction of the GTV coverage was necessary during online treatment planning for 3 fractions due to the dose constraint for the sacral plexus in the vicinity of the target. For the ATP plans the median GTV V_{35Gy} was 100% [93.9–100%] and the median GTV D_{mean} was 41.6 Gy [39.0–43.6 Gy] on the online planning MRI. On the post-radiation delivery MRI the median GTV V_{35Gy} was 100% [93.4–100%] and the median GTV D_{mean} was 41.5 Gy [38.9–43.7 Gy]. For 35 of the 50 fractions (70%) the GTV V_{35Gy} was 100% on the post-delivery MRI. Fig. 4 shows a visual example.

3.3. PTV margin analyses

The systematic and random intra-fraction displacement errors were respectively 0.31 and 0.27 mm in AP-direction, 0.54 and 0.23 mm in CC-direction and 0.22 and 0.33 mm in LR-direction. Only in AP-direction the group mean M (mean-of-mean) was significantly different from zero. The targets moved systematic in posterior direction during the individual MR-linac treatments. The group mean M was 0.33 mm in AP-direction, −0.07 mm in CC direction and 0.04 mm in LR-direction. The required PTV margin was estimated being 1.5 mm in LR-direction, 1.8 in AP-direction and 1.9 in CC-direction, respectively. Fig. 5 shows two examples of intra-fraction motion.

4. Discussion

MRI guided radiotherapy has been established during the last two decades. Broad clinical implementation has been realized for brachytherapy indications, mainly cervix and prostate [42–44]. Clinical gain of MRI guided brachytherapy in terms of local control and survival, not to the cost of treatment related morbidity, has been demonstrated for all stages of advanced cervical [45,46] and for prostate cancer [47]. In parallel, MRI guidance has become clinically available for external beam radiotherapy (EBRT) in 2014 with the combination of a 0.3 T MRI and 60 Cobalt radiotherapy device as realized in MRidian [48]. Since 2017 the combination of a 1.5T MRI and 7MV linear accelerator is available, bringing new opportunities for MRI guided high accuracy radiotherapy [29]. Since July 2018 this radiotherapy system is increasingly available for clinical routine treatments, starting in Europe and North-America with potential for global spread.

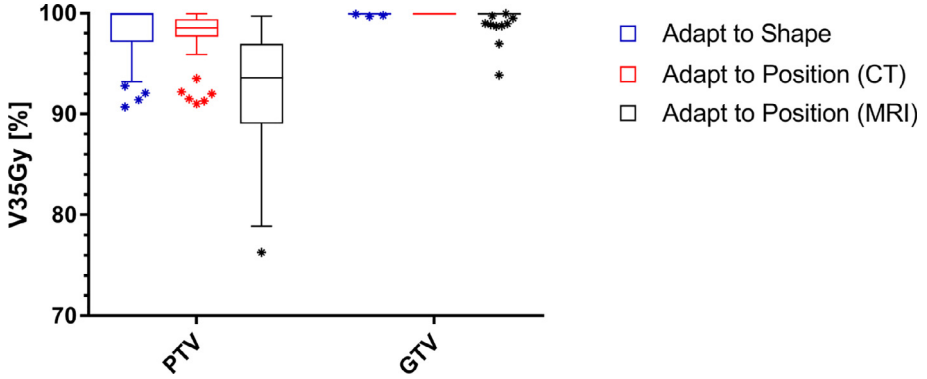

Fig. 2. Boxplot of the target dose coverage (N = 50 fractions) described as planning target volume (PTV) and gross target volume (GTV) V_{35Gy} in % for the adapted treatment plans. The bars show the upper and lower quartiles. The whiskers show the minimum and maximum values, excluding outliers (1.5 times the interquartile range) which are denoted with an asterisk. The target coverage for the adapt to shape plans is evaluated on the daily MRI. The target coverage for the adapt to position (CT) plans is evaluated on the pre-treatment CT and the target coverage for the adapt to shape (MRI) plans is evaluated on the daily MRI.

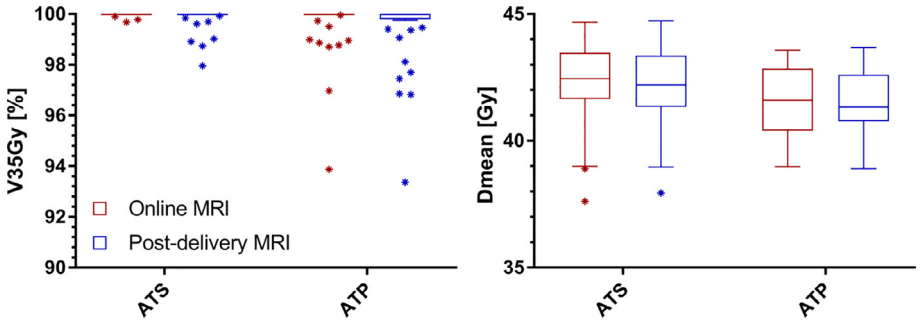

Fig. 3. Boxplot graph of the GTV coverage (N = 50) described as V_{35Gy} in % and D_{mean} in Gy for the clinically delivered (ATS) plans and the ATP plans. The bars show the upper and lower quartiles. The whiskers show the minimum and maximum values, excluding outliers (1.5 times the interquartile range) which are denoted with an asterisk. The coverage is evaluated on the daily MRI.

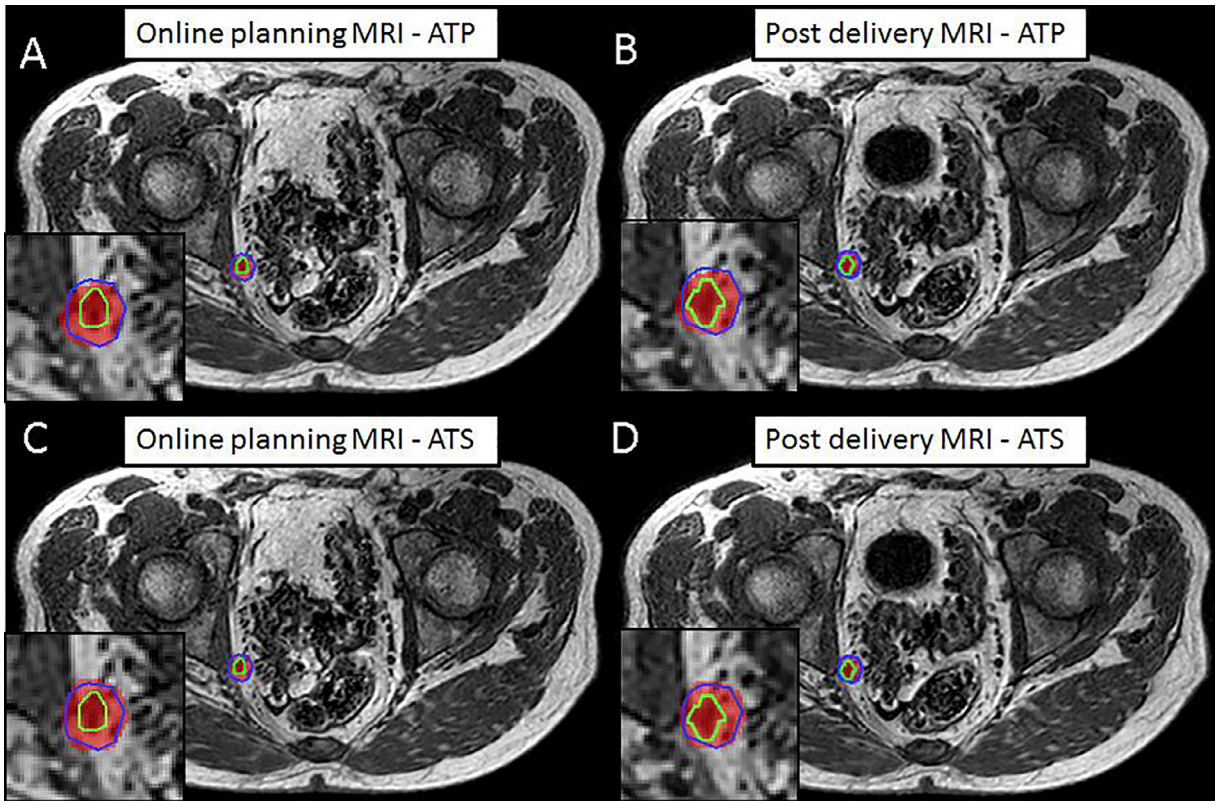

Fig. 4. Sample case with intra-fraction expansion of the bladder due to increased filling. Visible are the 35 Gy dose level (red), the PTV (blue) and the actual location of the GTV (green) for the ATP plan on the online planning MRI (A) and the post-delivery MRI (B) and the ATS plan on the online planning MRI (C) and the post-delivery MRI (D). The GTV V_{35Gy} remained 100% for the clinically delivered (ATS) plan. For this particular case the increasing bladder filling and GTV shift resulted in a small reduction of GTV V_{35Gy} from 100% to 97.5% with the ATP plan. (For interpretation of the references to colour in this figure legend, the reader is referred to the web version of this article.)

In our institute first clinical treatments on the 1.5T MR-linac were performed for patients with single oligometastatic lymph nodes in pelvis and para-aortic region. All nodes were well visible on the MRIs taken for treatment planning and position verification. The nodes were treated with SBRT (5×7 Gy) and the ATS online planning option, which allows to correct for inter-fraction motion by full online treatment planning based on the actual anatomy. All treatment planning aims were met for 40 out of 50 fractions. For 10 fractions the PTV coverage had to be sacrificed slightly in order to meet the hard constraints for OAR adjacent to the nodes and in 3 of these fractions the GTV coverage of the online plan was slightly less than intended (minimum 99.7%). In case the ATP workflow had been used online optimization would have been performed on the pre-treatment patient anatomy. In this case our treatment planning aims would have been met for only 19 out of 50 fractions and the GTV V_{35Gy} was reduced to 93.9% in the worst case. These clinical results show the additional dosimetric benefit of adaptive MRI-guided radiotherapy with online treatment planning based on the actual patient anatomy. In case of (hypo)-fractionated treatment approaches eventual inter-fraction anatomical changes can be accounted for. Because the ATS workflow is relatively labour-intensive compared to ATP, future studies will aim at predicting for which patients ATS would be most beneficial, and for whom ATP would also provide sufficient target coverage.

When evaluating the dose distributions of the online treatment plan on the anatomy of the post-treatment anatomy the chosen isotropic PTV margin of 3 mm turned out being adequate for treating single lymph nodes in the pelvis and para-aortic region on the

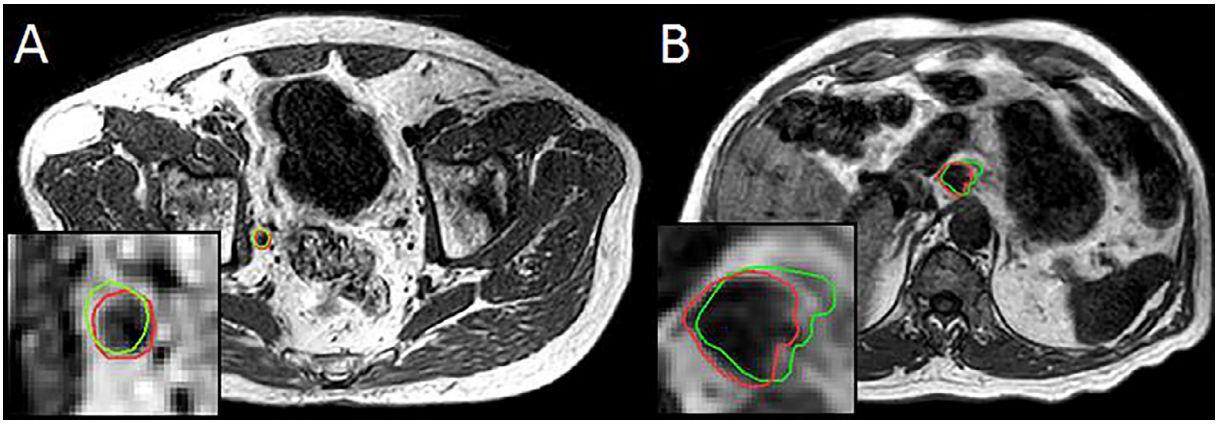

Fig. 5. Example cases intra-fraction target motion of lymph node oligometastases in the pelvic (A) and para-aortic (B) region. Visible are the post-delivery MRIs with the online planning GTV (green) and the GTV as observed on the post-delivery MRI (red). (For interpretation of the references to colour in this figure legend, the reader is referred to the web version of this article.)

MR-linac with the ATS treatment planning option. A limitation of this method is that potential system errors (e.g. MV-MR misalignments) are not accounted for. The PTV margin has to account for system errors as well as intra-fraction target motions and was therefore re-evaluated. Based on the Van Herk recipe [37] an isotropic PTV margin of 2 mm would have been adequate in all three directions in our series. However, noting the limitations of the recipe for SBRT treatments, very small tumors and higher density structures [38,49] we will still use a PTV margin of 3 mm for this particular indication in further treatments.

Within the group of oligometastatic nodal disease gain in terms of PTV margin reduction and less dose to the surrounding is especially expected for multiple metastatic lesions. In this situation daily treatment planning according to the daily anatomy might attenuate the effect of relative position shifts of the individual nodes relative to each other due to the changes of surrounding organs. Position shifts of pelvic lymph nodes are caused by movements and volume changes of the surrounding organs [50] and are not comparable to the intra-fraction motions of thoracic and abdominal lymph nodes, which are mainly affected by breathing [51,52]. Dosimetric gain of 1.5T MR-linac treatments is also expected in other tumor sites with potentially large inter and intra-fraction motion and substantial deformations such as prostate [53], cervix [54], and rectum [55].

A factor with potential impact on the PTV-margin is the time needed for an entire MR-linac treatment procedure. On-couch time for single lymph node SBRT is currently between 30 and 45 min in our clinical routine. The majority of this time is occupied by treatment planning and radiation delivery with IMRT, which is considerably longer than the few minutes being needed to deliver a VMAT plan as available for CBCT machines. However, when comparing the CBCT-linac single plan option for all treatment fractions with the daily treatment plan option of the 1.5T MR-linac we see dosimetric gain for target and/or OARs [36]. Further PTV margin reduction and dosimetric gain of MR-linac treatments is to be expected with intended machine and software updates. Less time consuming MRI protocols and treatment planning algorithms, VMAT instead of IMRT, tumor tracking during irradiation are among the options currently being developed.

Gain for our patients will include improved comfort through further hypo-fractionation with single fraction treatments on the MR-linac being aimed at as final goal. Due to the excellent soft tissue contrast of MRI treatment margins can be small, fiducial marker implantation as applied by others for position verification purposes can be avoided [22,23]. Clinical gain in terms of tumor related outcome such as local control, prolonged survival, later onset of systemic treatment as well as morbidity and quality of life is yet to be established.

Our study is limited by the relatively low number of cases available for the retrospective evaluation of ATS and ATP planning approaches and the margin analysis. The nodes, which are mainly originating from prostate cancer were detected by PSMA-PET, reflect small volume targets and essential volume reductions during the course of treatment are not expected [56]. Regardless of these limitations, the here presented findings correspond to earlier reported pre-clinical investigations [27,35] and validate our current treatment approach.

In conclusion, metastatic lymph nodes in the pelvis and para-aortic region can be treated on the 1.5T MR-linac within an acceptable time frame for the whole treatment procedure. We can effectively perform MRI based online treatment planning taking into account the actual patient anatomy and deliver the intended dose to the targets using small but adequate treatment margins. We feel that we are close to "See it and Zap it" with single fraction treatments including MRI based tumor tracking as final goal.

Acknowledgements

The authors wish to thank the Dutch Cancer Society for their financial support (grant 2015-0848).

Conflict of interest statement

The University Medical Center Utrecht MR-linac scientific project, including employment of multiple authors, has been partly funded by Elekta AB (Stockholm, Sweden) and Philips Medical Systems (Best, The Netherlands).

References

[1] Tree AC, Khoo VS, Eeles RA, Ahmed M, Dearnaley DP, Hawkins MA, et al. Stereotactic body radiotherapy for oligometastases. Lancet Oncol 2013;1:e28–37. https://doi.org/10.1016/S1470-2045(12)70510-7.

[2] De Bleser E, Tran PT, Ost P. Radiotherapy as metastasis-directed therapy for oligometastatic prostate cancer. Curr Opin Urol 2017;27:587–95. https://doi.org/10.1097/MOU.0000000000000441.

[3] Otake S, Goto T. Stereotactic Radiotherapy for Oligometastasis. Cancers (Basel) 2019;11:E133. https://doi.org/10.3390/cancers11020133.

[4] Hellman S, Weichselbaum RR. Importance of local control in an era of systemic therapy. Nat Clin Pract Oncol 2005;2:60–1. https://doi.org/10.1038/ncponc0075.

[5] Bouman-Wammes EW, van Dodewaard-De Jong JM, Dahele M, Cysouw MCF, Hoekstra OS, van Moorselaar RJA, et al. Benefits of using stereotactic body radiotherapy in patients with metachronous oligometastases of hormone-sensitive prostate cancer detected by [18F]fluoromethylcholine PET/CT. Clin

Genitourin Cancer 2017;15:e773–82. https://doi.org/10.1016/j.clgc.2017.03.009.
[6] Ost P, Reynders D, Decaestecker K, Fonteyne V, Lumen N, De Bruycker A, et al. Surveillance or metastasis-directed therapy for oligometastatic prostate cancer recurrence: a prospective, randomized, multicenter phase II trial. J Clin Oncol 2018;36:446–53. https://doi.org/10.1200/JCO.2017.75.4853.
[7] Steuber T, Jilg C, Tennstedt P, De Bruycker A, Tilki D, Decaestecker K, Zilli T, Jereczek-Fossa BA, Wetterauer U, Grosu AL, Schultze-Seemann W, Heinzer H, Graefen M, Morlacco A, Karnes RJ, Ost P. Standard of care versus metastases-directed therapy for PET-detected nodal oligorecurrent prostate cancer following multimodality treatment: a multi-institutional case-control study. Eur Urol Focus 2018. https://doi.org/10.1016/j.euf.2018.02.015 (Epub ahead of print).
[8] Timmerman RD, Bizekis CS, Pass HI, Fong Y, Dupuy DE, Dawson LA, et al. Local surgical, ablative, and radiation treatment of metastases. CA Cancer J Clin 2009;59:145–70. https://doi.org/10.3322/caac.20013.
[9] Aitken KL, Hawkins MA. Stereotactic body radiotherapy for liver metastases. Clin Oncol (R Coll Radiol) 2015;27:307–15. https://doi.org/10.1016/j.clon.2015.01.032.
[10] Shultz DB, Filippi AR, Thariat J, Mornex F, Loo Jr BW, Ricardi U. Stereotactic ablative radiotherapy for pulmonary oligometastases and oligometastatic lung cancer. J Thorac Oncol 2014;9:1426–33. https://doi.org/10.1097/JTO.0000000000000317.
[11] Comito T, Cozzi L, Clerici E, Campisi MC, Liardo RL, Navarria P, et al. Stereotactic Ablative Radiotherapy (SABR) in inoperable oligometastatic disease from colorectal cancer: a safe and effective approach. BMC Cancer 2014;14:619. https://doi.org/10.1186/1471-2407-14-619.
[12] Andratschke N, Alheid H, Allgäuer M, Becker G, Blanck O, Boda-Heggemann J, et al. The SBRT database initiative of the German Society for Radiation Oncology (DEGRO): patterns of care and outcome analysis of stereotactic body radiotherapy (SBRT) for liver oligometastases in 474 patients with 623 metastases. BMC Cancer 2018;18:283. https://doi.org/10.1186/s12885-018-4191-2.
[13] Scorsetti M, Comito T, Clerici E, Franzese C, Tozzi A, Iftode C, et al. Phase II trial on SBRT for unresectable liver metastases: long-term outcome and prognostic factors of survival after 5 years of follow-up. Radiat Oncol 2018;13:234. https://doi.org/10.1186/s13014-018-1185-9.
[14] Lancia A, Zilli T, Achard V, Dirix P, Everaerts W, Gomez-Iturriaga A, et al. Oligometastatic prostate cancer: the game is afoot. Cancer Treat Rev 2019;73:84–90. https://doi.org/10.1016/j.ctrv.2019.01.005.
[15] Palacios-Eito A, Béjar-Luque A, Rodríguez-Liñán M, García-Cabezas S. Oligometastases in prostate cancer: ablative treatment. World J Clin Oncol 2019;10:38–51. https://doi.org/10.5306/wjco.v10.i2.38.
[16] Chance WW, Nguyen QN, Mehran R, Welsh JW, Gomez DR, Balter P, et al. Stereotactic ablative radiotherapy for adrenal gland metastases: factors influencing outcomes, patterns of failure, and dosimetric thresholds for toxicity. Pract Radiat Oncol 2017;7:e195–203. https://doi.org/10.1016/j.prro.2016.09.005.
[17] Ippolito E, D'Angelillo RM, Fiore M, Molfese E, Trodella L, Ramella S. SBRT: a viable option for treating adrenal gland metastases. Rep Pract Oncol Radiother 2015;20:484–90. https://doi.org/10.1016/j.rpor.2015.05.009.
[18] Moghul M, Somani B, Lane T, Vasdev N, Chaplin B, Peedell C, et al. Detection rates of recurrent prostate cancer: 68Gallium (Ga)-labelled prostate-specific membrane antigen versus choline PET/CT scans. A systematic review. Ther Adv Urol 2019;11. https://doi.org/10.1177/1756287218815793. 1756287218815793.
[19] Fowler J, Chappell R, Ritter M. Is alpha/beta for prostate tumors really low? Int J Radiat Oncol Biol Phys 2001;50:1021–31. https://doi.org/10.1016/S0360-3016(01)01607-8.
[20] Ponti E, Lancia A, Ost P, Trippa F, Triggiani L, Detti B, et al. Exploring all avenues for radiotherapy in oligorecurrent prostate cancer disease limited to lymph nodes: a systematic review of the role of stereotactic body radiotherapy. Eur Urol Focus 2017;3:538–44. https://doi.org/10.1016/j.euf.2017.07.006.
[21] Taylor LG, Canfield SE, Du XL. Review of major adverse effects of androgen-deprivation therapy in men with prostate cancer. Cancer 2009;115:2388–99. https://doi.org/10.1002/cncr.24283.
[22] Detti B, Bonomo P, Masi L, Doro R, Cipressi S, Iermano C, et al. Stereotactic radiotherapy for isolated nodal recurrence of prostate cancer. World J Urol 2015;33:1197–203. https://doi.org/10.1007/s00345-014-1427-x.
[23] Muldermans JL, Romak LB, Kwon ED, Park SS, Olivier KR. Stereotactic body radiation therapy for oligometastatic prostate cancer. Int J Radiat Oncol Biol Phys 2016;95:696–702. https://doi.org/10.1016/j.ijrobp.2016.01.032.
[24] Pasqualetti F, Panichi M, Sainato A, Matteucci F, Galli L, Cocuzza P, et al. [(18)F] Choline PET/CT and stereotactic body radiotherapy on treatment decision making of oligometastatic prostate cancer patients: preliminary results. Radiat Oncol 2016;11:9. https://doi.org/10.1186/s13014-016-0586-x.
[25] Laliscia C, Fabrini MG, Delishaj D, Morganti R, Greco C, Cantarella M, et al. Clinical outcomes of stereotactic body radiotherapy in oligometastatic gynecological cancer. Int J Gynecol Cancer 2017;27:396–402. https://doi.org/10.1097/IGC.0000000000000885.
[26] Siva S, Bressel M, Murphy DG, Shaw M, Chander S, Violet J, et al. Stereotactic abative body radiotherapy (SABR) for oligometastatic prostate cancer: a prospective clinical trial. Eur Urol 2018;74:455–62. https://doi.org/10.1016/j.eururo.2018.06.004.
[27] Winkel D, Kroon PS, Werensteijn-Honingh AM, Bol GH, Raaymakers BW, Jürgenliemk-Schulz IM. Simulated dosimetric impact of online replanning for stereotactic body radiation therapy of lymph node oligometastases on the 1.5T MR-linac. Acta Oncol 2018;3:1–8. https://doi.org/10.1080/0284186X.2018.1512152.
[28] Noel CE, Parikh PJ, Spencer CR, Green OL, Hu Y, Mutic S, et al. Comparison of onboard low-field magnetic resonance imaging versus onboard computed tomography for anatomy visualization in radiotherapy. Acta Oncol 2015;54:1474–82. https://doi.org/10.3109/0284186X.2015.1062541.
[29] Raaymakers BW, Jürgenliemk-Schulz IM, Bol GH, Glitzner M, Kotte ANTJ, van Asselen B, et al. First patients treated with a 1.5 T MRI-Linac: clinical proof of concept of a high-precision, high-field MRI guided radiotherapy treatment. Phys Med Biol 2017;62:L41–50. https://doi.org/10.1088/1361-6560/aa9517.
[30] Werensteijn-Honingh AM, Kroon PS, Winkel D, Aalbers EM, Van Asselen B, Bol GH, et al. Feasibility of stereotactic radiotherapy using a 1.5 T MR-linac: multi-fraction treatment of pelvic lymph node oligometastases. Radiother Oncol 2019;134:50–4. https://doi.org/10.1016/j.radonc.2019.01.024.
[31] Winkel D, Bol G, Werensteijn-Honingh A, Kiekebosch I, Hes J, Intven M, et al. Dose escalation and hypofractionation for SBRT of lymph node oligometastases on the 1.5T MRI-Linac. Radiother Oncol 2018;127:S443–4. https://doi.org/10.1016/S0167-8140(18)31158-7 (conference abstract).
[32] Henke L, Kashani R, Yang D, Zhao T, Green O, Olsen L, et al. Simulated online adaptive magnetic resonance-guided stereotactic body radiation therapy for the treatment of oligometastatic disease of the abdomen and central thorax: characterization of potential advantages. Int J Radiat Oncol Biol Phys 2016;96:1078–86. https://doi.org/10.1016/j.ijrobp.2016.08.036.
[33] Heerkens HD, Reerink O, Intven MPW, Hiensch RR, van den Berg CAT, Crijns SPM, et al. Pancreatic tumor motion reduction by use of a custom abdominal corset. Phys Imaging Radiat Oncol 2017;2:7–10. https://doi.org/10.1016/j.phro.2017.02.003.
[34] Winkel D, Kroon PS, Hes J, Bol GH, Raaymakers BW, Jürgenliemk-Schulz IM. Automated full-online replanning of SBRT lymph node oligometastases for the MR-linac. Radiother Oncol 2017;123:S904. https://doi.org/10.1016/S0167-8140(17)32195-3 (conference abstract).
[35] Winkel D, Bol G, Werensteijn-Honingh A, Kiekebosch I, Van Asselen B, Intven M, et al. Evaluation of plan adaptation strategies for stereotactic radiotherapy of lymph node oligometastases using online magnetic resonance image guidance. Phys Imaging Radiat Oncol 2019;9:58–64. https://doi.org/10.1016/j.phro.2019.02.003.
[36] Winkel D, Bol G, Werensteijn-Honingh A, Intven M, Eppinga W, van Asselen B, et al. Dosimetric benefit of the first clinical SBRT of lymph node oligometastases on the 1.5T MR-linac. ESTRO 2019 (conference abstract).
[37] van Herk M, Remeijer P, Rasch C, Lebesque JV, et al. The probability of correct target dosage: dose-population histograms for deriving treatment margins in radiotherapy. Int J Radiat Oncol Biol Phys 2000;47:1121–35.
[38] Gordon JJ, Siebers JV. Convolution method and CTV-to-PTV margins for finite fractions and small systematic errors. Phys Med Biol 2007;52:1967–90. https://doi.org/10.1088/0031-9155/52/7/013.
[39] de Boer JCJ, Heijmen BJM. A protocol for the reduction of systematic patient setup errors with minimal portal imaging workload. Int J Radiat Oncol Biol Phys 2001;50:1350–65.
[40] Tijssen RHN, Philippens MEP, Saulson ES, Glitzner M, Chugh B, Wetscherek A, et al. MRI commissioning of 1.5T MR-linac systems – a multi-institutional study. Radiother Oncol 2019;132:114–20. https://doi.org/10.1016/j.radonc.2018.12.011.
[41] Stroom JC, Heijmen BJ. Geometrical uncertainties, radiotherapy planning margins, and the ICRU-62 report. Radiother Oncol 2002;64:75–83.
[42] Tanderup K, Viswanathan A, Kirisits C, Frank SJ. MRI-guided brachytherapy. Semin Radiat Oncol 2014;24:181–91. https://doi.org/10.1016/j.semradonc.2014.02.007.
[43] Sturdza A, Pötter R, Fokdal LU, Haie-Meder C, Tan LT, Mazeron R, et al. Image guided brachytherapy in locally advanced cervical cancer: improved pelvic control and survival in RetroEMBRACE, a multicenter cohort study. Radiother Oncol 2016;120:428–33. https://doi.org/10.1016/j.radonc.2016.03.011.
[44] Pötter R, Tanderup K, Kirisits C, de Leeuw A, Kirchheiner K, Nout R, et al. The EMBRACE II study: the outcome and prospect of two decades of evolution within the GEC-ESTRO GYN working group and the EMBRACE studies. Clin Transl Radiat Oncol 2018;9:48–60. https://doi.org/10.1016/j.ctro.2018.01.001.
[45] Rijkmans EC, Nout RA, Rutten IH, Ketelaars M, Neelis KJ, Laman MS, et al. Improved survival of patients with cervical cancer treated with image-guided brachytherapy compared with conventional brachytherapy. Gynecol Oncol 2014;135:231–8. https://doi.org/10.1016/j.ygyno.2014.08.027.
[46] Tanderup K, Fokdal LU, Sturdza A, Haie-Meder C, Mazeron R, van Limbergen E, et al. Effect of tumor dose, volume and overall treatment time on local control after radiochemotherapy including MRI guided brachytherapy of locally advanced cervical cancer. Radiother Oncol 2016;120:441–6. https://doi.org/10.1016/j.radonc.2016.05.014.
[47] Nguyen PL, Chen MH, Zhang Y, Tempany CM, Cormack RA, Beard CJ, et al. Updated results of magnetic resonance imaging guided partial prostate brachytherapy for favorable risk prostate cancer: implications for focal therapy. J Urol 2012;188:1151–6. https://doi.org/10.1016/j.juro.2012.06.010.
[48] Fischer-Valuck BW, Henke L, Green O, Kashani R, Acharya S, Bradley JD, et al. Two-and-a-half-year clinical experience with the world's first magnetic resonance image guided radiation therapy system. Adv Radiat Oncol 2017;2:485–93. https://doi.org/10.1016/j.adro.2017.05.006.

[49] Witte MG, van der Geer J, Schneider C, Lebesque JV, van Herk M. The effects of target size and tissue density on the minimum margin required for random errors. Med Phys 2004;31:3068–79. https://doi.org/10.1118/1.1809991.

[50] Wiersema L, Borst G, Nakhaee S, Peulen H, Wiersma T, Kwint M, et al. First IGRT results for SBRT bone and lymph node oligometastases within the pelvic region. Radiother Oncol 2017;123:S1006. https://doi.org/10.1016/S0167-8140(17)32273-9 (conference abstract).

[51] Pantarotto JR, Piet AH, Vincent A, van Sörnsen de Koste JR, Senan S. Motion analysis of 100 mediastinal lymph nodes: potential pitfalls in treatment planning and adaptive strategies. Int J Radiat Oncol Biol Phys 2009;74:1092–9. https://doi.org/10.1016/j.ijrobp.2008.09.031.

[52] Yorke E, Xiong Y, Han Q, Zhang P, Mageras G, Lovelock M, et al. Kilovoltage imaging of implanted fiducials to monitor intrafraction motion with abdominal compression during stereotactic body radiation therapy for gastrointestinal tumors. Int J Radiat Oncol Biol Phys 2016;95:1042–9. https://doi.org/10.1016/j.ijrobp.2015.11.018.

[53] McPartlin AJ, Li XA, Kershaw LE, Heide U, Kerkmeijer L, Lawton C, et al. MRI-guided prostate adaptive radiotherapy – a systematic review. Radiother Oncol 2016;119:371–80. https://doi.org/10.1016/j.radonc.2016.04.014.

[54] Kerkhof EM, van der Put RW, Raaymakers BW, van der Heide UA, Jürgenliemk-Schulz IM, Lagendijk JJ. Intrafraction motion in patients with cervical cancer: the benefit of soft tissue registration using MRI. Radiother Oncol 2009;93:115–21. https://doi.org/10.1016/j.radonc.2009.07.010.

[55] Nijkamp J, Swellengrebel M, Hollmann B, de Jong R, Marijnen C, van Vliet-Vroegindeweij C, et al. Repeat CT assessed CTV variation and PTV margins for short- and long-course pre-operative RT of rectal cancer. Radiother Oncol 2012;102:399–405. https://doi.org/10.1016/j.radonc.2011.11.011.

[56] Schippers MG, Bol GH, de Leeuw AA, van der Heide UA, Raaymakers BW, Verkooijen HM, et al. Position shifts and volume changes of pelvic and para-aortic nodes during IMRT for patients with cervical cancer. Radiother Oncol 2014;111:442–5. https://doi.org/10.1016/j.radonc.2014.05.013.